Sustainable Hybrid Route to Renewable Methacrylic Acid via Biomass-Derived Citramalate

Yuxiao Wu[1,2], Manish Shetty[1], Kechun Zhang[1,2,3*] Paul J. Dauenhauer[1,2*]

[1] Department of Chemical Engineering and Materials Science, University of Minnesota, 421 Washington Ave. SE, Minneapolis, MN 55455, USA

[2] Center for Sustainable Polymers, Department of Chemistry, 208 Smith Hall, 207 Pleasant Street SE, Minneapolis, MN, USA, 55455.

[3] School of Engineering, Westlake University, Zhejiang, Hangzhou, Xihu, 18 Shilongshan Road Cloud Town, China.

*Corresponding author: zhangkechun@westlake.edu.cn, hauer@umn.edu

Abstract. Combined chemical technologies of microbial fermentation and thermal catalysis provides a hybrid process for sustainable manufacturing of biorenewable sugar-derived monomers for plastics. In this work, methacrylic acid (MAA), a target molecule for the polymer industry, was produced from biomass-derived glucose through the intermediate molecule, citramalic acid. The biosynthetic pathway engineered in *E. coli* produced citramalic acid intermediate with a high yield (91% of theoretical maximum) from glucose by overexpressing citramalate synthase, removing downstream degradation enzyme 3-isopropylmalate dehydratase, and optimizing the fermentation medium. Thermal heterogeneous catalysis converted the citramalate intermediate to methacrylic acid (MAA) via decarboxylation and dehydration. A selectivity of ~71% for the production of MAA and its intermediate α-hydroxybutyric acid was achieved at a temperature of 250 °C and an acidity of 1.0 mol acid/mol citramalate. An alumina catalyst was found to enhance selectivity to MAA in a single reactor pass from 45.6% in the absence of catalyst to 63.2%. This limited selectivity to MAA was attributed to equilibrium between MAA and α-hydroxybutyric acid, but overall process selectivity to MAA was shown to be higher upon separation and recycle of reaction intermediates. The highest overall glucose-to-MMA yield was 0.65 mole MAA per mole glucose. A process flow diagram was proposed of the hybrid route for the conversion of glucose to the final end product, methacrylic acid, for poly(methyl methacrylate) (PMMA).

1.0 Introduction. The development of biobased renewable materials is essential in addressing the environmental and social issues of climate change and plastic waste[1,2,3]. In addition to producing novel bio-monomers or bio-polymers, a parallel effective approach is the drop-in replacement strategy, whereby existing and commercially available monomers are synthesized from biomass feedstocks.[4,5,6,7,8] In the polymer industry, the physical and chemical properties of these polymers have been known for decades, and these modern plastics play an essential role in society. For example, biobased polyethylene already exists via bioethanol production, which produces low-cost two-carbon alcohols that can be dehydrated to ethylene.[9,10] However, besides bioethanol-derived monomers, few processes exist for cost effective, efficient, and environmentally benign manufacturing of large-volume commodity monomers.

Methacrylic acid (MAA) has been a target molecule in the polymer industry as its ester, methyl methacrylate (MMA), is an important monomer produced at three billion kilograms annually for many advanced materials.[11] It can be polymerized with itself into poly(methyl methacrylate) (PMMA), also known as acrylic glass,[12] which has the functions of being transparent, durable, and UV tolerant, and is mainly used as a glass substitute.[13] Other copolymers of MMA, such as styrene methyl methacrylate (SMMA) and methyl methacrylate-butadiene-styrene (MBS), have better properties in terms of moisture absorption and impact strength,[14,15] making them widely used in packaging, homeware, and medical appliances.

The dominant industrial process for MMA production occurs through the acetone-cyanohydrin (ACH) reaction.[16] This process in its current form utilizes toxic reactants, such as hydrogen cyanide,

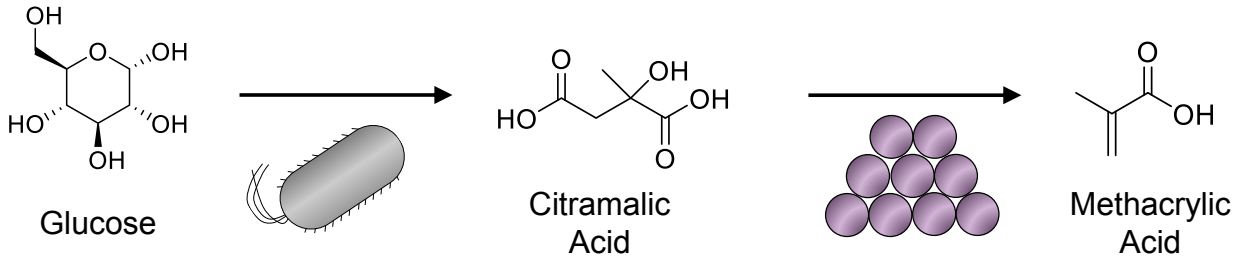

Scheme 1. Hybrid fermentation and thermocatalysis to produce Methacrylic acid (MAA) from glucose through citramalic acid.

as well as produces toxic cyanide intermediates. Other commercial processes, such as ethylene-based 'alpha process', isobutene oxidation, and isobutane process are all based on non-renewable fossil-fuel-derived feedstock.[11] There is an increasing demand for MAA with its predicted annual market expected to exceed $8 billion USD by 2025.[17] Thus, both industry and academic research groups have put more effort in designing bio-renewable routes to MAA and MMA[18].

Due to their acute toxicity in both eukaryotes and prokaryotes, few examples have been reported for the direct production of MAA or MMA through microbial fermentation of biomass.[19] Other proposed attempts to utilize biomass feedstock have mainly focused on using biobased chemicals within existing chemical processes. For example, methanol, ethanol, isobutene, and isobutyric acid can all be used as starting materials for MMA production,[17] all of which can be synthesized biorenewably through direct fermentation (ethanol)[20], via synthesis gas from biomass gasification (methanol)[21,22], or from dehydration of fermentation products (isobutene from isobutanol)[23,24].

Another biorenewable approach to manufacture MAA and MMA combines hybrid chemical routes of microbial fermentation and thermochemical catalysis to utilize biomass-derived sugars[25]. Fermentation of glucose has already been developed to manufacture chemical intermediates such as itaconic acid in high yield (up to 0.58 g/g glucose)[26,27,28]; itaconic acid can be decarboxylated to form methacrylic acid[29,30]. Other isomers of itaconic acid, mesaconic acid and citraconic acid, have also been considered as potential intermediates in hybrid routes to MAA through a similar decarboxylation mechanism.[17] Among the three isomers, the bioproduction of itaconic acid using fungi such as *Aspergillus terreus* and other strains has already achieved commercial status[31,32]. Recently, Tehrani et al. reported a high yield of 0.58 g itaconic acid/g glucose and maximal production rate of nearly 1.0 g/L-h.[33] In bacterial system of *Escherichia coli* (henceforth referred to as *E.coli*), the yields towards itaconic acid were significantly lower with the highest reported yield of 0.11 g/g glucose using acetate as starting material.[34] High yields of bio-based intermediates mesaconic acid and citraconic acid have not yet been demonstrated. The catalytic strategies include the chemical decarboxylation of intermediates such as itaconic acid to MAA. These studies have reported high selectivity to MAA (> 90%) from itaconic acid, albeit at a maximum yield of 50%.[30,35] Therefore, it is desirable to maximize the yields of the final product, MAA, in bio-based hybrid routes, particularly from fermentation-derived intermediates like citramalate, which can be obtained at high yield from glucose.

Herein, the conversion of glucose to methacrylic acid was achieved through a combined biotechnological fermentation with heterogeneous catalysis hybrid approach (**Scheme 1**). First, *E. coli* strains were optimized to maximize the yield of the intermediate, citramalic acid, an alternative diacid which can be fermented at higher yield than existing diacids, such as itaconic or mesaconic acid. This was achieved through a systematic approach of gene knockouts to minimize the yield of side products in competing pathways. Efficient bio-production of citramalate was previously achieved in a fed-batch process with glucose (172 g/L in total) and yeast extract (1.4 g/L).[36] Lactate dehydrogenase and pyruvate formate lyase was removed to block the metabolism of pyruvate, one of the precursors to form citramalate. Similarly another approach is to reduce the metabolism of the

other precursor, acetyl-CoA, through eliminating acetate formation.[37] The *pta*, *ackA* and *poxB* gene deletions were found to be critical to reducing acetate accumulation during aerobic growth. In this study, we examined the effect of removing 3-isopropylmalate dehydratase by deleting genes coding for its subunits from *E. coli* which metabolizes citramalate in the leucine biosynthesis pathway. We discovered that with optimal medium, the knockout strain achieved high yield (91% of theoretical maximum), compared to 20% in a previous study with minimal salt medium.[38] Next, a systematic heterogeneous catalyst and reaction parameter design approach controlled for decarboxylation and dehydration of citramalate to form MAA. Reaction conditions including acidity and reaction temperatures were first optimized to identify the optimum reaction conditions. Finally, catalysts were tested to study the influence of catalysis on the selectivity towards desired MAA and undesired side products. Overall, we demonstrate that high yields of MAA can be achieved from glucose through the approach of combining fermentation to citramalate and heterogeneous catalysis for decarboxylation.

2.0 Experimental Methods. The overall chemical route of glucose to citramalate and eventually methacrylic acid was evaluated through two separate experiments: (i) biotechnological fermentation of glucose to citramalate, and (ii) heterogeneous catalysis for citramalate decarboxylation. Methods for each chemical technology and the associated experiments and chemical analysis are described in the sequence of process chemistry.

2.1 Microbe Design and Preparation. Microbial strains (*E. coli*) used for fermentation were derived from the wild type *E. coli* K-12 strain BW25113. *E. coli* strains used for transformation were purchased from Stratagene (XL10-Gold). The *leuC* and *leuD* knockout strains along with P1 phage of ackA were obtained from the Keio collection.[39] Phage was used to transfect the corresponding strains for construction of targeted knockout strains.[40] Kanamycin markers were removed after the strains were transformed with pCP20 plasmids. Colony PCR was performed after transformation to verify the knockouts. The *E. coli* strains were grown in glass test tubes at 37 °C in 2xYT rich medium (16 g/L tryptone, 10 g/L yeast extract, and 5 g/L NaCl) supplemented with appropriate antibiotics (100 mg/L ampicillin or 50 mg/L kanamycin).

Chemicals used in the study were purchased from Sigma-Aldrich, unless otherwise specified. All plasmids and primers used in the study are listed in Table S1. PCR reactions were carried out with Q5 High-Fidelity DNA polymerase (New England Biolabs) according to the manufacturer's instructions. FastDigest restriction enzymes were purchased from Thermo Scientific. Sequences of all the plasmids constructed were verified by restriction mappings and DNA sequencing.

2.2 Fermentation Process. Conical flasks (125 mL) were used for all 48-hour fermentations. Overnight cultures (200 µL) were transferred into the fermentation medium, which contained 5.0 ml M9 minimal media supplemented with 5.0 g/L yeast extract, 20 g/L glucose, 5.0 µM coenzyme B12, and 100 mg/L ampicillin. Isopropyl-β-D-thiogalactoside (IPTG) was added at a final concentration of 0.4 mM to induce the overexpression of introduced genes for the production of (R)-citramalate. 0.5 g $CaCO_3$ was added to all flasks as a buffer. Fermentations were carried out in a shake incubator set at 30 °C, rotated at 250 rpm. Error bars indicated the standard deviation obtained from two independent experiments by picking different colonies for fermentation. Fermentation products were quantified by the parameter titer (see equation 1 below).

$$Titer\ (g/L) = \frac{mass\ of\ product\ formed\ in\ g}{volume\ of\ fermentation\ broth\ in\ L} \quad (1)$$

The titer values represented the concentration of the product in the fermentation broth and is another metric for the yield of fermentation products for comparison with existing literature.

2.3 Catalyst Pretreatment and Characterization. Chemicals used in the study were purchased from Sigma-Aldrich, unless otherwise specified. (±)-Potassium citramalate monohydrate ($K_2C_5H_7O_5 \cdot H_2O$), purchased from VWR International, was used as a starting substrate for the batch-phase reactions and used without further treatments. Itaconic acid, citraconic acid, acetic acid, α-Hydroxyisobutyric acid, pyruvic acid, propanoic acid, and methacrylic acid were used as

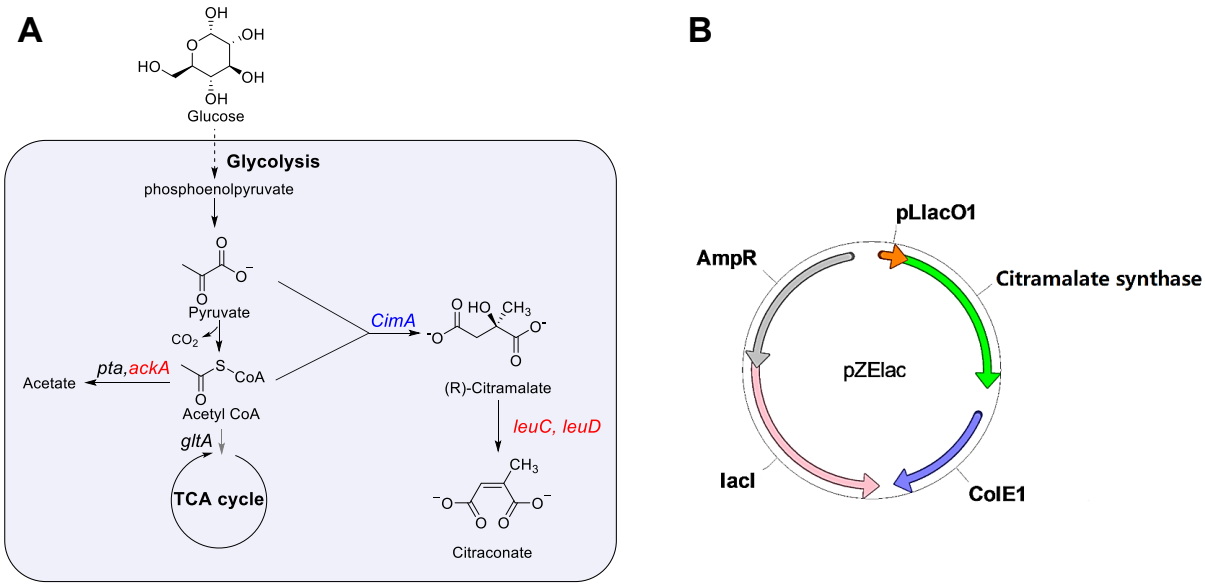

Figure 1. (A) Biosynthetic pathway for (R)-citramalate in *E. coli*. Pyruvate and acetyl-CoA, two major metabolites derived from glycolysis pathway, are condensed by citramalate synthase (CimA) to produce (R)-citramalate. Knock out of key enzyme prevents downstream conversion of citramalate (LeuC, LeuD) or reduces acetate accumulation (ackA). **(B)** Plasmid map of the pZElac_mjCimA plasmid. It has a replication origin (initiation of replication) from ColE1, pLlacO1 promoter (drives transcription of the target gene), lac repressor LacI (inhibits the metabolism of lactose), and ampicillin resistant marker (antibiotic selectable marker). It carries gene *CimA* encoding the citramalate synthase.

organic standards for product analysis. Several commercial catalysts were utilized for the batch-phase conversion of potassium citramalate to products, including 10% Pd/C (Acros Organics), 5% Pd/C, 1% Pd/C, 5% Pd/Al_2O_3, 5% Ru/C, 10% Pt/C (STREM Chemicals), carbon, and gamma-alumina (STREM Chemicals). The supported metal catalysts were treated in H_2 at 300 °C for three hours prior to reaction. Hydrochloric acid (HCl) was used without any further treatment.

2.4 Catalytic Conversion of Potassium Citramalate. The catalytic conversion of potassium citramalate was conducted in a 100 ml high-pressure batch reactor (PARR Instruments). In a typical experiment, 242 mg of potassium citramalate monohydrate (1.0 mmol) was dissolved in 30 ml of deionized (DI) water. 80 mg pretreated catalyst was added into the solution and loaded inside the glass liner of the batch reactor. The reactor was then heated to the set temperature. The reactor was pressurized with 600 Psi nitrogen gas after it reaches the set temperature. The timer for the reaction (time zero) was started when the reactor has been pressurized. At the end of the reaction, the reactor was quenched by cooling with immersion in an ice bath. The reactor was depressurized at 4 °C to prevent loss of products in the vapor phase.

2.5 Chemical Analysis of Catalytic Products. Both the fermentation mixtures and catalytic products were quantified with the aid of high-performance liquid chromatography (HPLC, Agilent 1260 Infinity). The HPLC was equipped with the Aminex HPX 87H column (Bio-Rad, USA), and all products were detected by the refractive-index and the DAD detectors. The mobile phase was H_2SO_4 (concentration 5 mM) at a flow rate of 0.6 ml/min. Proton ^1H spectral analysis was performed on a AM-400 Bruker Avance III HD NMR spectrometer, and data were processed using MestraNova NMR software. The conversion of reactant and selectivity to the products were quantified using the following formulae.

$$Conversion\ (mol\%) = \frac{moles\ of\ reactant\ consumed}{moles\ of\ initial\ reactant} \times 100 \qquad (2)$$

$$Selectivity\ (mol\%) = \frac{moles\ of\ product\ formed}{moles\ of\ reactant\ consumed} \times 100 \qquad (3)$$

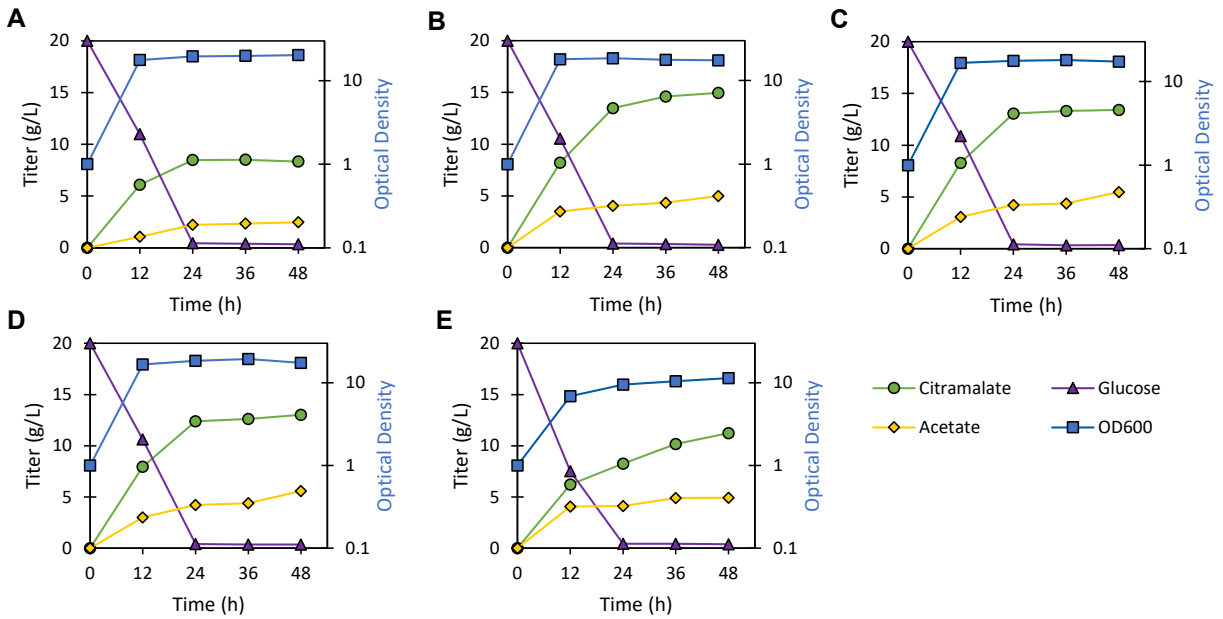

Figure 2. De novo production of (R)-citramalate from glucose in *E. coli*. (A) CM0: Wild type BW25113 (F') with cimA (B)CM1: ΔleuC strain with CimA overexpressed by the pZE plasmid (C) CM2: ΔleuD strain with CimA overexpressed by the pZE plasmid (D) CM3: ΔleuCΔleuD strain with CimA overexpressed by the pZE plasmid. (E) CM4: ΔleuCΔackA strain with CimA overexpressed by the pZE plasmid.

3.0 Results and Discussion. The efficiency of the hybrid chemical route to methacrylic acid (MAA) and ultimately methyl methacrylate (MMA) depends on the independent catalyst and biocatalyst technologies to achieve high selectivity. As shown via economic sensitivity analysis within full process techno-economic analyses[41,42,43], the loss of feedstock carbon due to side reactions in large-scale commodity processes is the single most impactful metric for economic viability of a chemical technology. For this reason, the two sequential reactions, fermentation of sugars to citramalate and decarboxylation of citramalate, are presented in order with a focus on catalyst performance.

3.1. Metabolic pathway design for maximizing the yield of (R)-citramalate. The metabolic pathway for producing (R)-citramalate in *E. coli* is depicted in **Figure 1A**. The heterologous expression of the key enzyme, citramalate synthase, from *Methanococcus jannaschii* (CimA; EC 2.3.1.182) in metabolically engineered *E. coli* allowed the efficient de novo production of (R)-citramalate from glucose. The two intermediates in the glycolysis pathway, pyruvate and acetal-CoA, combine to form (R)-citramalate from glucose, catalyzed by the citramalate synthase enzyme.

Since *M. jannaschii* is a thermophilic archaeon, the CimA isolated from *M. jannaschii* has the highest activity at 70 °C. To increase both the activity and stability at moderate temperatures, directed evolution of this citramalate synthase was conducted by Atsumi and Liao.[44] CimA3.7, the variant which was expressed in *E.coli* for hyperproduction of 1-propanol and 1-butanol, was found to have the most improved activity and was also insensitive to feedback inhibition by isoleucine. It was also shown that this variant is also active during fermentation at *E. coli*'s optimum growth temperature (37 °C). CimA3.7 was inserted into the plasmid pZElac with pLlacO1 promoter and replication origin from ColE1. The detailed plasmid map is shown in **Figure 1B**. Specifically, the plasmid had a replication origin (initiation of replication) from ColE1, placO1 promoter (drives transcription of the target gene), lac repressor LacI (inhibits the metabolism of lactose), and ampicillin resistant marker (antibiotic selectable marker). It carried gene CimA that encodes the citramalate synthase.

The fermentation capability of different *E. coli* strains containing citramalate synthase to convert

glucose to (R)-citramalate is depicted in **Figure 2**. First, the wild type strain CM0 (BW25113 pZE–mjCimA) was subjected to fermentation in a batch process with 20 g/L glucose feed. The highest titer of 8.49 g/L citramalate was detected in the broth after 24 hours (**Figure 2A**). The citramalate pathway from *M. jannaschii* was successfully introduced into *E. coli*, and the heterologous gene *cimA* was functional in *E. coli in vivo*.

Further metabolic engineering increased the accumulation of citramalate in fermentation. The first approach to elevate the citramalate titer eliminated the downstream pathway of citramalate metabolism in *E. coli*. The 3-isopropylmalate dehydratase (leuCD) catalyzes the dehydration of citramalate producing citraconate. The enzyme is a complex of two subunits, the large (leuC) and the small (leuD) subunit. The deletion of the gene *leuC* in the fermentation strain resulted in a titer of 14.9 g/L after 48 hours (**Figure 2B**). The deletion of the gene *leuD* in the fermentation strain resulted in a titer of 13 g/L after 48 hours (**Figure 2C**). In both cases, we observed a higher rate in citramalate production compared to the wild type BW25113. However, the deletion of both *leuC* and *leuD* genes did not result in a higher citramalate titer (**Figure 2D**). We hypothesize that the deletion of one of the subunits prevents 3-isopropylmalate dehydratase from functioning and therefore prevents the downstream conversion of citramalate.

In previous literature, the effect of deleting *leuC* or *leuD* was studied under a different fermentation condition. The use of XC medium alone did not support *E. coli* growth, thus 0.2 g/L leucine was added to the medium to restore cell growth. 1 g/L citramalate was produced from 5 g/L glucose feed. No difference in citramalate production titer was observed compared to the wild type. In our fermentation medium, 5 g/L yeast extract was added which supplies nutrients such as minerals and amino acids. The highest OD during fermentation with strain CM1 (ΔleuC) reached 20.4, which was more than twice the OD of fermentation using wild type MG1655 with same initial glucose concentration (20 g/L). The key differences between the two results were accounted for the fermentation medium contents, as we utilized a more optimized fermentation condition. Calcium carbonate (100 g/L) was added at the start of the fermentation as a pH buffer. BW25113 derived from MG1655 was also the wild type strain that is more suitable for industrial level fermentation. Thus, with increased citramalate production titer and yield, we concluded that the effect of removing 3-isopropylmalate dehydratase by deleting *leuC* or *leuD* was significant with optimized medium content.

We also noticed an increase in the acetate accumulation during the fermentation process with all the fermentation strains. Acetate could slow down cell growth at concentrations as low as 0.5 g/L.[45] This was also observed in previous studies in citramalate production from fermentation.[37] Acetate is an undesirable byproduct potentially formed from acetyl-CoA in aerobic fermentation environment. Acetal-CoA is also the key substrate for citramalate production. This pathway consists of the enzymes, phosphate acetyltransferase (pta) and acetate kinase (ackA). Therefore, the next approach to increase the citramalate titer was attempted by reducing the generated acetate side product. To achieve this, the gene *ackA* was deleted alongside *leuC*. From the fermentation results (**Figure 2E**), this deletion did not produce a

Table 1. Comparison of fermentation processes for relevant diacid production

Diacid	Microorganism	Substrate	Titer [g/L]	Yield [mol/mol]	Reference
Itaconic acid	*A. terreus*	Glucose	129	0.80	51
Itaconic acid	*U. maydis*	Glucose	220	0.46	33
Itaconic acid	*E. coli*	Glucose	32	0.77	47
Mesaconic acid	*E. coli*	Glucose	23	0.64	48
Citraconic acid	-	-	-	-	-
Citramalic acid	*E. coli*	Glucose	54	0.78	37
Citramalic acid	*E. coli*	Glucose	15	0.91	This Study

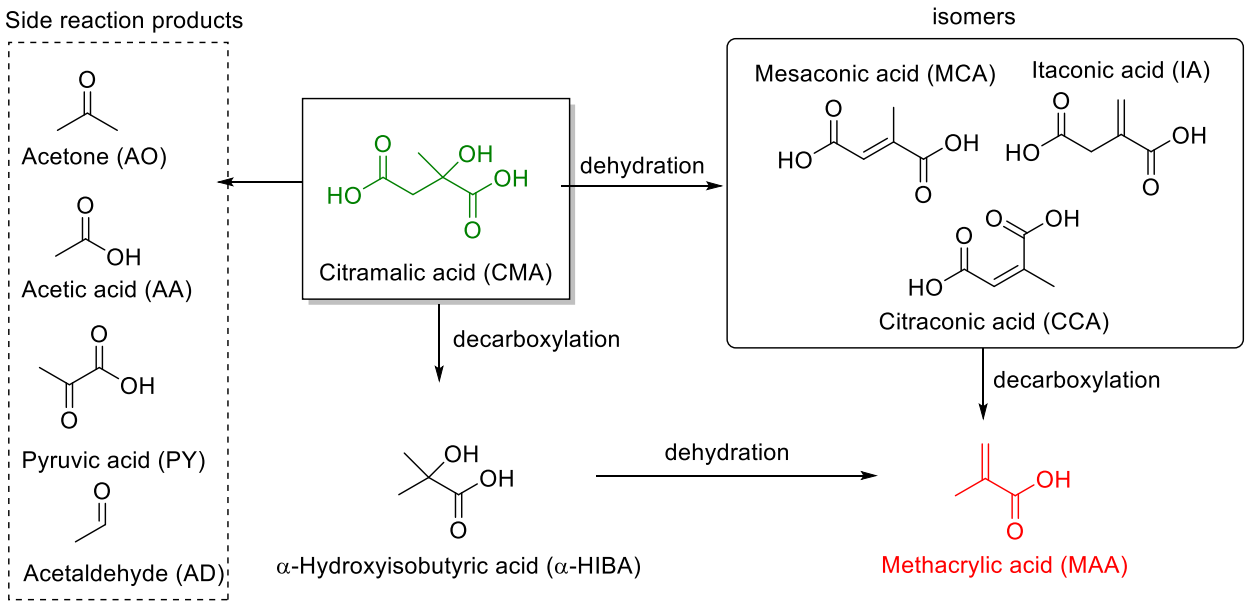

Figure 3. Intermediates and side products of the decarboxylation and dehydration of citramalic acid.

significant decrease in the acetate amount in the fermentation broth. However, it resulted in slower cell growth and much lower citramalate production rate compared with the strain with only *leuC* deleted. Acetate could also be generated from other catabolic reaction pathways thus the deletion of *ackA* gene alone was not enough to reduce acetate accumulation.[46]

Overall, the highest citramalate titer obtained from our fermentation was 14.9 g/L, corresponding to a yield of 0.91 mol/mol glucose (batch process with 20 g/L as initial concentration of glucose and 5 g/L yeast extract). The yield is 91% of theoretical maximum considering glucose as the carbon source, since the rest of the materials should be used to sustain cell growth. The mol/mol ratio of citramalic acid produced from *E.coli* fermentation is higher compared to other diacid products (80%). The comparison for the highest yield strains is shown in **Table 1**[47,48,38].

Among all proposed diacid intermediates in a hybrid route to methacrylic acid, itaconic acid can be produced from glucose with the highest titer (220 g/L), albeit from *Ustilago maydis*, a fungus less economically viable in large-scale commodity chemical production.[33] The yield and production rate is also lower compared to what was achieved with *A. terreus* (0.80 mol/mol and 1.15 g/L/h as compared to 0.92 mol/mol and 0.52 g/L/h in the current study).[49] Alternatively, the fermentation of citramalate evaluated herein and elsewhere[36,37] utilizes *E. coli*, a bacterium commonly utilized in large-volume chemical manufacturing as it is fast growing with capability for modification.[50] The use of *E. coli* here allowed for the modification of the natural glycolysis pathway with only one enzyme to be introduced, producing citramalate at the yield of 91% which is significantly above the highest yield of itaconic acid (80%) produced from *A. terreus,* as mentioned earlier.[51]

3.2. Conversion of citramalic acid to methacrylic acid (MAA). Catalytic experiments evaluated the production of methacrylic acid (MAA) from citramalate through thermocatalytic routes. As shown in **Figure 3**, citramalic acid can first undergo dehydration to form the isomers of itaconic acid, mesaconic acid, or citraconic acid, depending on which neighboring proton participates in dehydration (and the resulting stereochemistry). Subsequent decarboxylation forms MAA, as has already been shown for itaconic acid decarboxylation[29]. Alternatively, our experiments indicated the following pathways, whereby citramalic acid can undergo decarboxylation to form α-hydroxyisobutyric acid (α-HIBA), which can undergo further dehydration to form MAA. The additional decarboxylation of MAA and the cleavage of C-C bonds of citramalic acids lead to formation of several side products that include acetone, acetic acid, pyruvic acid, and

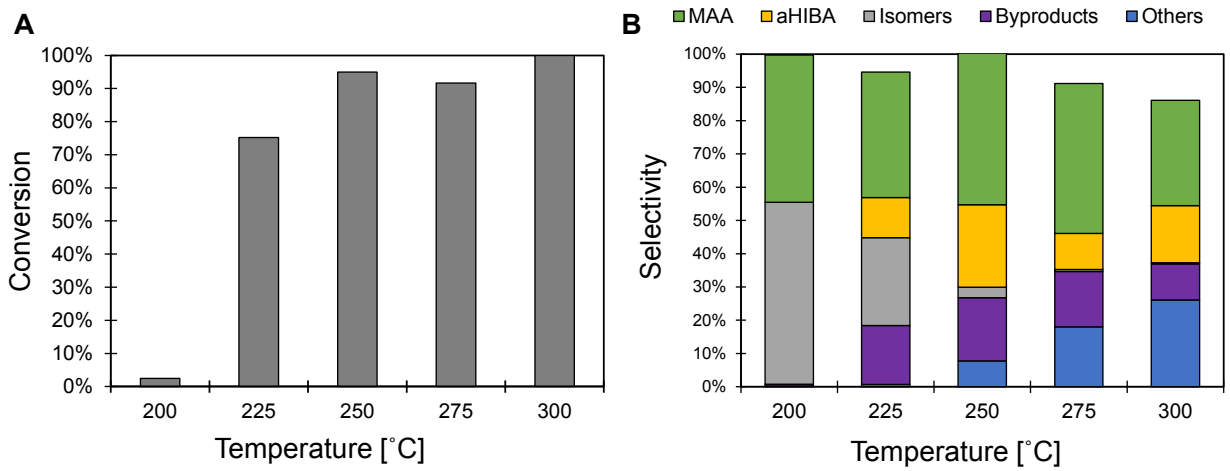

Figure 4. Temperature effect on conversion of citramalate **(A)** and selectivity to products **(B)**. At temperatures below 250 ˚C, conversion was low (reaction at 200 ˚C for six hours). At temperatures above 250 ˚C, more byproduct formation was observed. Reaction conditions: P of 600psi N_2, reaction time of one hour. Starting material: (±)-Potassium citramalate monohydrate 1.0 mmol in 30 ml H_2O. 1:1 HCl:MAA. Products observed included Methacrylic acid (MAA), α-Hydroxyisobutyric acid (α-HIBA), isomers including itaconic acid, mesaconic acid, citraconic acid, and byproducts (Acetic acid, pyruvic acid, acetone and acetaldehyde). Others: Unidentified products detected in HPLC.

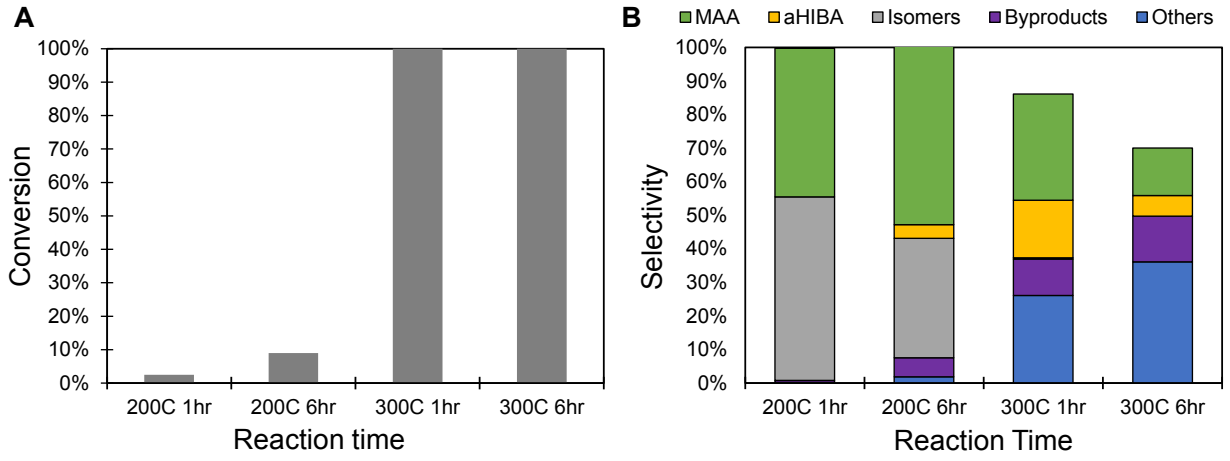

Figure 5. Effect of reaction time on conversion of citramalate **(A)** and selectivity to products **(B)**. Longer reaction time at low temperature resulted in higher conversion and selectivity towards Methacrylic acid (MAA). Longer reaction time at high temperature resulted in more side products and decreasing selectivity towards MAA. Reaction conditions: P of 600 psi N_2. Starting material: (±)-Potassium citramalate monohydrate 1.0 mmol in 30 ml H_2O, 1:1 HCl. MAA is Methacrylic acid; α-HIBA is α-Hydroxyisobutyric acid. Isomers include: Itaconic acid, mesaconic acid, citraconic acid. Byproducts: Acetic acid, pyruvic acid, acetone and acetaldehyde. Others: Unidentified products detected in HPLC

acetaldehyde, all of which are economically undesirable.

Initial experiments evaluated the effect of temperature on the conversion of potassium citramalate (**Figure 4A**) and selectivity to products such as MAA in an aqueous-phase batch reactor. Citramalate was used in the salt form, because it was the final product after being extracted from the fermentation broth. The reactant mixture consisted of 0.033 M potassium citramalate with 1.0 molar equivalent of HCl (*vide infra*), which was reacted between 200 – 300 ^{o}C for one hour. At 200 ^{o}C the conversion was less than 3%. As shown in **Figure 4B**, the selectivity towards MAA increased from ~38% to ~46% on a molar basis with increasing temperature from 225 to 250 ^{o}C. With a further

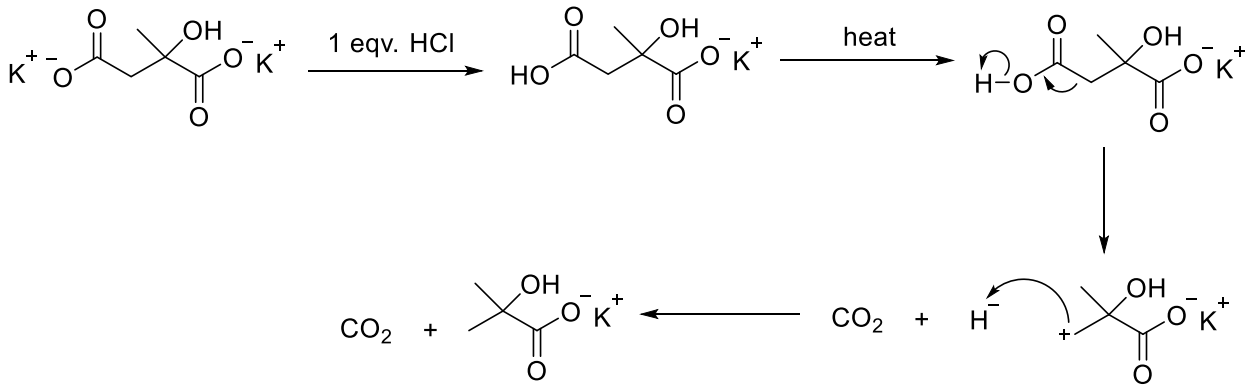

Scheme 2. Decarboxylation of potassium citramalate with hydrochloric acid.

increase in temperature to 300 °C, the selectivity towards MAA reduced to nearly 32%. Additionally, the selectivity towards α-HIBA remained between 10-26% across all temperatures, excluding 200 °C. We note that the comparisons were deliberately made at similar conversion values and of interest to commercial practice (between 70-100%).

During the HCl-catalyzed reaction of citramalate, the selectivity to itaconic acid, mesaconic acid, and citraconic acid isomers by dehydration accounted for ~26% at 225 °C and reduced to zero at higher temperatures. Notably, the selectivity towards unknown undesired byproducts increased from ~1% at 225 °C to ~26% at 300 °C. Overall, we identified 250 °C to be the optimum temperature to maximize the selectivity towards the pathway of MAA formation involving decarboxylation followed by dehydration that showed a maximum yield of ~70% at 250 °C (both MAA and α-HIBA).

The reaction time of potassium citramalate monohydrate with hydrochloric acid was also evaluated by comparing the extent of conversion (**Figure 5A**) and selectivity to products (**Figure 5B**) after one hour and six hours at both 200 and 300 °C. After one hour at 200 °C, the conversion of citramalate was <3%. Only MAA and diacid isomers were observed, indicating that at low temperature the formation of MAA goes through the dehydration of citramalate to form itaconic,

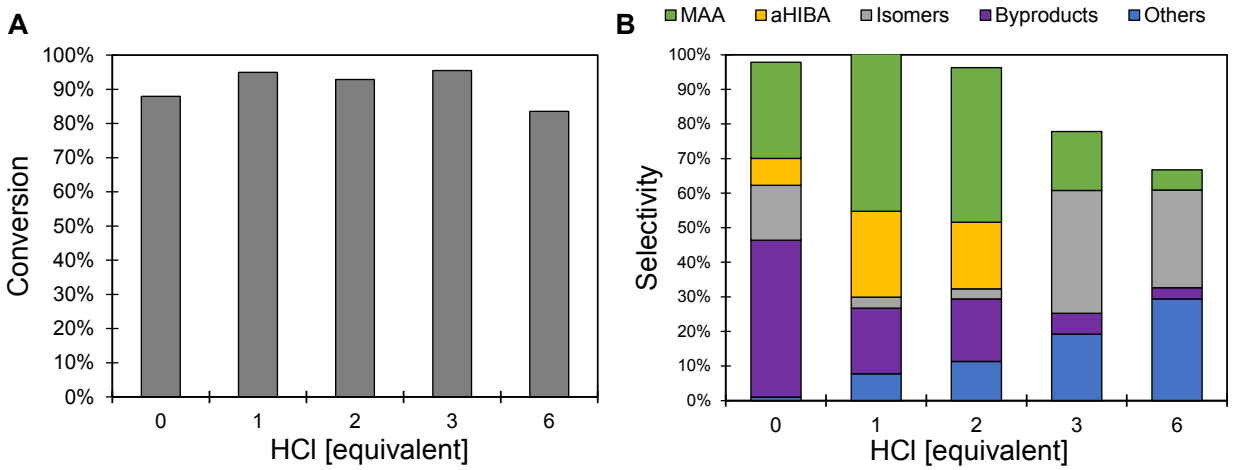

Figure 6. The effect of acid addition on decarboxylation of citramalate monohydrate conversion **(A)** and selectivity to products **(B)**. As acidity increases (pH decreases), more carbon was converted to undesirable products during the reaction. Reaction conditions: T of 250 °C, P of 600 psi N_2, reaction time of one hour. Starting material: (±)-Potassium citramalate monohydrate 1.0 mmol in 30 ml H_2O. MAA: Methacrylic acid ; α-HIBA: α-Hydroxyisobutyric acid. Isomers: Itaconic acid, mesaconic acid, citraconic acid. Byproducts: Acetic acid, pyruvic acid, acetone and acetaldehyde. Others: Unidentified products detected in HPLC.

mesaconic, and citraconic acid isomers. Therefore, formation of MAA likely occurs through the decarboxylation of diacid isomers at this lower temperature of 200 ºC. The conversion of citramalate increased to ~9% after 6 hours concomitant with higher selectivity towards MAA. In addition, α-HIBA was observed at this relatively higher conversion, possibly from the hydration of MAA or from the decarboxylation of citramalate. At 300 ºC, the conversion of citramalate increased to almost 100% and several new products were observed. The selectivity to both α-HIBA and MAA decreased significantly between one hour and six hours of reaction. This decrease in selectivity is accompanied by increased selectivity of "other" products and lower selectivity to MAA and other liquid products (total product selectivity < 100%), suggesting that secondary decarboxylation and decomposition reactions lead to undesired side products and likely formation of CO_2 which was not measured.

The effect of acidity on the conversion of potassium citramalate (0.033 M) was next studied (**Figure 6**) at 250 ºC, to identify the optimal ratio of acid to reactant on product selectivity. We first note that all comparisons were made at conversion between 80-100% on a molar basis (**Figure 6A**). As shown in **Figure 6B**, the absence of hydrochloric acid addition produces large quantities of undesirable byproducts (>50%) and only minimal MAA (<30%). With the addition of 1.0 equivalent HCl, the selectivity of MAA significantly improved to ~46%. On further HCl addition from 1.0 equivalent to 6.0 equivalent HCl, the selectivity towards MAA reduced from ~46% to ~6%. This established that 1.0 HCl equivalent was the optimum acidity desired for the highest selectivity towards MAA. In addition, the optimum selectivity towards α-HIBA was also achieved at 1.0 HCl equivalent. Taken together, we identified 1.0 HCl equivalent to be the optimum acidity to maximize the selectivity towards the pathway of MAA formation involving the pathway that goes through decarboxylation to form α-HIBA followed by dehydration to form MAA, showing a maximal yield of ~70% at 250 ºC. When the diacid isomers (itaconic acid, mesaconic acid and citraconic acid) were also included as desirable intermediates along the dehydration/decarboxylation pathway to MAA, the yield increased to ~74%.

The optimal acid loading of 1.0 equivalent of HCl per citramalate is consistent with the mechanism of salt formation protecting carboxylate groups from decarboxylation. For example, as shown for lactic acid dehydration, the addition of cations such as Na^+ or K^+ suppresses the decarboxylation reaction, thereby permitting dehydration to occur for the formation of acrylic acid.[30] In the case of diacids such as citramalate, the addition of 1.0 equivalent HCl addition are likely to lead to ion exchange between protons (H^+) and potassium ions (K^+) of potassium citramalate,

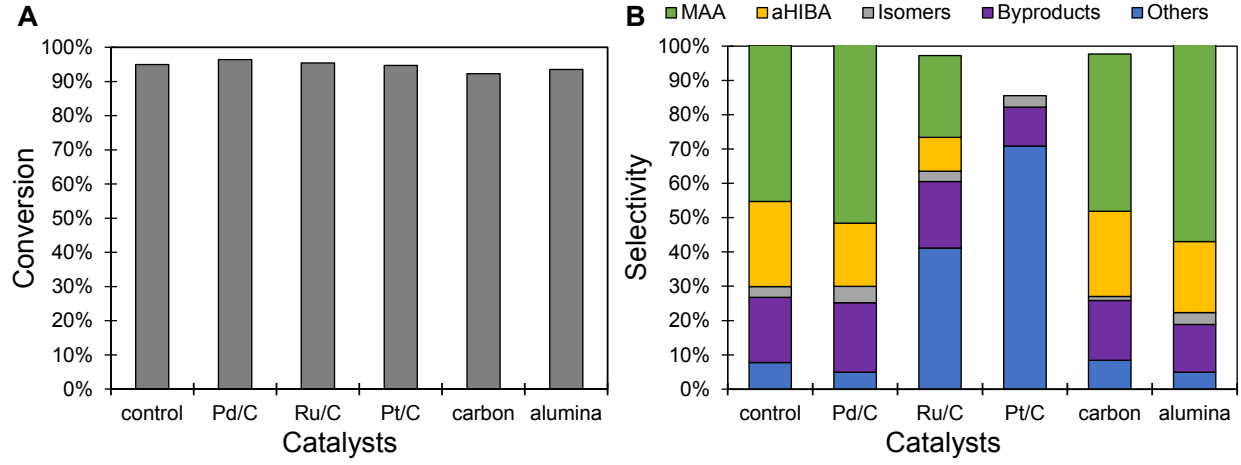

Figure 7. The effect of catalysts on decarboxylation of citramalate monohydrate conversion **(A)** and selectivity to products **(B)**. Reaction conditions: T of 250˚C, P of 600psi N_2, reaction time of one hour. Starting material: (±)-Potassium citramalate monohydrate 1.0 mmol in 30 ml H_2O. HCl 1:1. MAA: Methacrylic acid ; α-HIBA: α-Hydroxyisobutyric acid. Isomers: Itaconic acid, mesaconic acid, citraconic acid. Byproducts: Acetic acid, pyruvic acid, acetone and acetaldehyde. Others: Unidentified products detected on HPLC

leading to the predominant formation of monopotassium citramalate.[52] As depicted in **Scheme 2**, this yields selective decarboxylation of the carboxylic acid group leading to the formation of α-HIBA that then undergoes further dehydration to form MAA. On further addition of HCl, the ion exchange likely forms citramalic acid which can undergo further decarboxylation reactions to form side products (**Figure 2**). In addition, the reduction in the selectivity of liquid products from ~100% at 1.0 equivalent HCl to ~70% at 6.0 equivalent HCl was consistent with the loss of products as CO_2 in the gas phase in line with the increased decarboxylation.

Citramalate decarboxylation was further evaluated using solid acid catalysts and supported metal catalysts including Pd/C, Ru/C, Pt/C as shown in **Figure 7**. Experiments were conducted at high conversion (250 ºC, 600 psi N_2) of interest to commercial application. We note that the carbon support did not have an effect on increasing MAA selectivity (**Figure 7B**) when compared with the control (no catalyst). γ-Alumina increased the selectivity towards MAA from ~46% to ~63%, implicating the acid sites in catalyzing the decarboxylation and dehydration reaction. Doubling the alumina catalyst amount did not further increase the selectivity. HZSM-5 catalysts with varying acidity (SiO_2/Al_2O_3 ratios) were also investigated as catalysts for the decarboxylation reaction, and did not lead to any significant changes in MAA selectivity. In summary, increasing the acidity of the solid acid catalyst did not further increase MAA selectivity. Unsurprisingly, on the other hand, decreasing the acidity resulted in slightly lower MAA selectivity (59.3%) as well as less dehydration product formation.

Among the supported metal catalysts, the addition of Pd/C (2.67 g/L) increased the selectivity towards MAA from ~46% to ~55%, while decreasing the yield of α-HIBA. The effect of Pd loading on MAA selectivity was next studied. The catalytic performance of Pd/C with different Pd loading (1%,5%,10%) showed little effect on MAA selectivity (50.6% - 54.6%). Next, the nature of the supports was varied. Palladium on a neutral silica support (Pd/SiO_2) also showed similar MAA selectivity as Pd/C, showing the limited role played by both the neutral C and SiO_2 supports on the reaction pathway. Then, we investigated the influence of acidic supports on product selectivity. Both 5 wt% $Pd/\gamma\text{-}Al_2O_3$ and $\gamma\text{-}Al_2O_3$ resulted in similar MAA selectivity. We note that physical mixtures of Pd and $\gamma\text{-}Al_2O_3$ also did not result in any further increase in MAA selectivity (Table S4).Taken together, the addition of Pd to acidic $\gamma\text{-}Al_2O_3$ did not exhibit any synergistic effect leading to an increase in selectivity.

Alternatively, both Ru/C and Pt/C produced large quantities of byproducts not previously observed in homogeneously catalyzed decarboxylation reactions; Pt/C also generated significant quantities of gas-phase byproducts such as acetone and acetaldehyde. Overall, Pd/C and Al_2O_3 catalysts showed great promise to improve MAA selectivity from citramalate.

As Pd has an affinity for double bonds, the delocalized structure of the a-carboxylate and the unsaturation potentially coordinates to the metal surface, which stabilizes the intermediates during the decarboxylation reaction from diacid isomers to MAA.[53] Therefore, Pd facilitates the dehydration/decarboxylation reaction pathway. Any addition of acid catalysts (γ-alumina or HZSM-5) promotes the dehydration reaction. Thus, the reactions readily go through the decarboxylation/dehydration pathway when solid acid catalysts were present.

The plateauing of catalytic performance towards MAA selectivity posed a question whether there exists an equilibrium limit to formation of MAA, specifically the equilibrium of α-HIBA dehydration to MAA in the reaction mixture. To characterize equilibrium, MAA in water alone was added to the reactor and allowed to react to equilibrium at varying temperatures. The equilibrium constants (K_{eq}) were calculated for each temperature using equation (4) and plotted in **Figure 8**. In these experiments, the reaction proceeded to form α-HIBA until a fixed ratio of [MAA]/[α-HIBA] was achieved, even when subsequent side reactions occurred. With this measured ratio at each temperature, the reaction enthalpy (ΔH_{rxn} of 44.1 kJ mol^{-1}) and entropy (ΔS_{rxn} of 93.8 J mol^{-1} K^{-1}) were determined from the slope and intercept of the plot of $\ln K_{eq}$ versus 1/T (Van't Hoff equation) shown in equation (5).

$$K_{eq} = \frac{[MAA][H_2O]}{[HIBA]} \qquad (4)$$

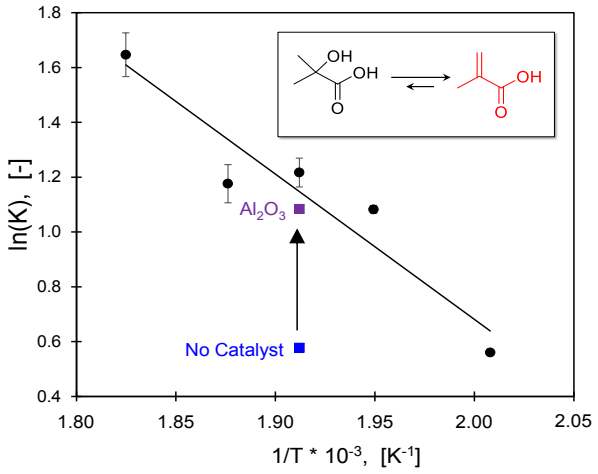

Figure 8. Equilibrium formation of methacrylic acid (MAA) and water from α-hydroxy-isobutyric acid. The dehydration of α-hydroxy-isobutyric acid (α-HIBA) to form MAA was measured at five temperatures at equilibrium (●) to determine the equilibrium constant K with associated ΔH_{rxn} of 44.1 kJ mol^{-1} and ΔS_{rxn} of 93.8 J mol^{-1} K^{-1}. For comparison, the conversion of citramalic acid without a catalyst (■, blue) at 250 ºC for one hour did not achieve equilibrium, but introduction of an alumina catalyst (■, purple) at 250 ºC for one hours did equilibrate MAA and α-HIBA, thereby achieving maximum yield of MAA product.

$$lnK_{eq} = -\frac{\Delta H}{RT} + \frac{\Delta S}{R} \qquad (5)$$

Increased reaction temperature favors dehydration to form MAA. At 250 ºC, the predicted ratio of [MAA]/[α-HIBA] is 3.4 indicating that complete conversion to MAA is prohibited by equilibrium.

For comparison, the conversion of citramalic acid without a catalyst at 250 ºC for one hour did not achieve equilibrium; as shown in **Figure 8**. Specifically, this experiment (depicted in blue) produced a ratio of [MAA]/[HIBA] inconsistent with equilibrium mixtures. However, introduction of an alumina catalyst at 250 ºC for one hour increased the catalytic rate of dehydration to equilibrate MAA and α-HIBA, thereby achieving maximum yield of MAA product at 250 ºC. This is further evidence that the overall catalytic reaction of citramalic acid can only achieve an equilibrium-limited yield of MAA. Further increasing the MAA yield at equilibrium could occur by increasing the reaction temperature, but this was already shown (**Figure 5**) to increase byproduct formation. For this reason, a process solution is required to remove MAA from the reaction mixture and promote further conversion of α-HIBA to MAA.

In previous studies, the existing biobased route to methacrylic acid was based on catalytic decarboxylation of itaconic acid. The highest

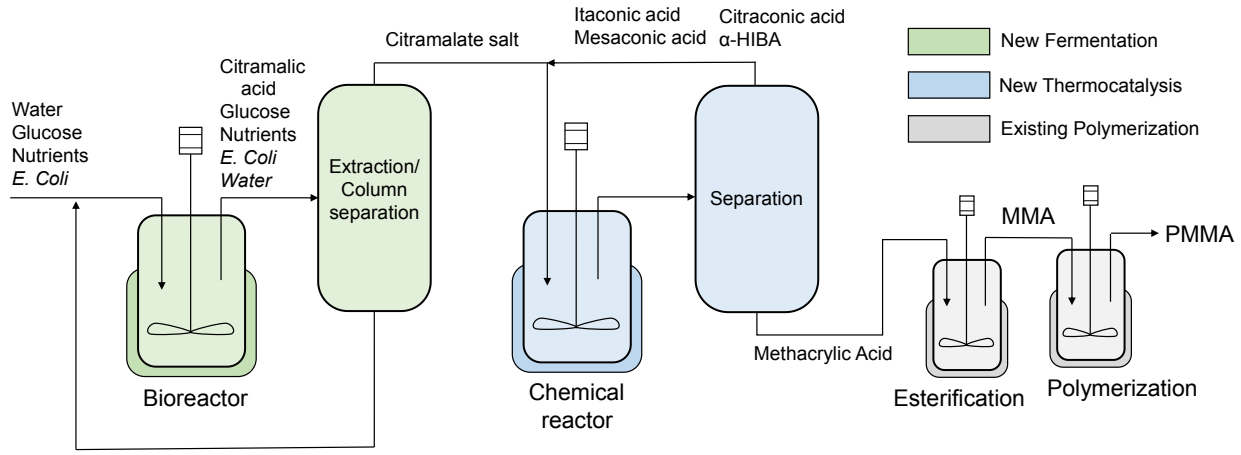

Figure 9. A proposed process flow diagram for sustainable hybrid production of poly(methyl methacrylate) from glucose. Water, glucose, metabolically engineered *E. coli*, and nutrients are added to the bioreactor to start the fermentation process to produce citramalic acid. Citramalic acid is then separated by an extraction/column separation process to obtain the salt form citramalate. Citramalate salt is then used as the substrate for the chemical reactor to produce methacrylic acid (MAA). Reaction intermediates such as diacids and α-hydroxyisobutyric acid are then recycled to further react to MAA. The resulting MAA is then separated via extraction, esterified to methyl methacrylate, and used as the monomer for poly(methyl methacrylate) (PMMA).

reported selectivity to MAA was 75% when reacting in supercritical water in plug flow reactors.[54] In similar batch reaction conditions (T<300ºC, P<600Psi, reaction time < 3h), the selectivity to MAA lowered to ~40%.[30] We demonstrated that our system was very close to reaching the equilibrium limit. As α-HIBA was also present in the IA to MAA process, the α-HIBA/MAA equilibrium we reported would also limit the yield of MAA in that process.

The utility of the considered hybrid pathway through citramalate to methacrylic acid will ultimately be determined by the chemistry's integration within a chemical process and its associated economic potential. As depicted in **Figure 9**, the process will include an upstream fermenter which combines glucose, water, engineered *E. coli*, and nutrients to produce an aqueous stream of citramalic acid. Subsequent purification steps, including filtration and extraction, will produce citramalate salt (see page 8 of Supporting Information). The impurities will be mainly crystalized ammonium chloride and small amounts of other organic acid salts. These impurities could potentially be removed by vacuum heating or ion exchange column separation to obtain citramalate salt with high purity. We note that *in situ* product recovery could be implemented, similar to methods used to produce itaconic acid.[55] After purification, bio-derived citramalate is the starting material for the dehydration/decarboxylation reaction to produce MAA. The uncompleted reaction products, (itaconic acid, citraconic acid, mesaconic acid and α-HIBA) could be recycled for further decarboxylation/dehydration to produce MAA. By this approach, the overall process yield of MAA will exceed the single pass reactor selectivity to MAA. Finally, the down-stream processing and isolation of MAA can be recreated from the existing patented literature on the extraction process.[29] The manufactured MAA is then be esterified to form MMA and polymerized to form PMMA for use in industrial and consumer applications. Detailed process design, techno-economic analysis, and life-cycle analysis of this general process design is the focus of future work.

4.0 Conclusions. Combined hybrid chemical routes of microbial fermentation and thermal catalysis to utilize biomass-derived sugars to form biorenewable monomers is a promising sustainable route for green manufacturing of plastics. In this work, the conversion of biomass-derived glucose to methacrylic acid, a target molecule for the polymer industry, was studied through a combined biotechnological fermentation with heterogeneous catalysis hybrid approach. A biosynthetic pathway was used to make citramalic acid intermediate with a high yield (91% of theoretical maximum) after simple gene editing and fermentation medium optimization. Next, a thermal catalysis approach was utilized to convert the citramalate intermediate to methacrylic acid (MAA). A temperature of 250 ^{o}C and an acidity of 1.0 mol acid/mol citramalic acid were identified as optimal for the production of MAA and its intermediate α-hydroxybutyric acid with selectivity values approaching ~70%. High temperature and high acidity led to secondary decarboxylation reactions forming CO_2 and consequently low liquid product yields. A Pd/C catalyst enhanced selectivity to MAA from 45.6% in the absence of catalyst to 63.2%. Other catalysts including Ru/C and Pt/C led to formation of a large amount of side products. Combining the highest yields of the biochemical and thermocatalytic routes, the glucose-to-MAA overall yield was 0.65 mol MAA/mol glucose (assuming recycle of α-HIBA). Finally, we proposed an integrated chemical process of the hybrid route for the conversion of glucose to the polymer, PMMA.

Acknowledgements. This research was supported the NSF Center for Sustainable Polymers at the University of Minnesota, a National Science Foundation supported Center for Chemical Innovation (CHE-1901635). M.S. is partially supported by the farm families of Minnesota and their corn check-off investment through the Minnesota Corn Growers Association.

Supporting Information. The supporting information is available free of charge online and includes a description of strains and plasmids, summaries of reaction conditions of decarboxylation of citramalate, 1H-NMR of citramalic acid, HPLC spectra of reaction compounds, and catalyst characterization.[56]

Keywords. Methacrylic acid, citramalate, fermentation, catalysis, decarboxylation, dehydration

References

(1) Alonso, D. M.; Hakim, S. H.; Zhou, S.; Won, W.; Hosseinaei, O.; Tao, J.; Garcia-Negron, V.; Motagamwala, A. H.; Mellmer, M. A.; Huang, K.; Houtman, C. J.; Labbé, N.; Harper, D. P.; Maravelias, C. T.; Runge, T.; Dumesic, J. A. Increasing the Revenue from Lignocellulosic Biomass: Maximizing Feedstock Utilization. *Sci. Adv.* **2017**, *3* (5). https://doi.org/10.1126/sciadv.1603301.

(2) Law, K. L.; Starr, N.; Siegler, T. R.; Jambeck, J. R.; Mallos, N. J.; Leonard, G. H. The United States' Contribution of Plastic Waste to Land and Ocean. *Sci. Adv.* **2020**, *6* (44). https://doi.org/10.1126/sciadv.abd0288.

(3) Hillmyer, M. A. The Promise of Plastics from Plants. *Science (80-.).* **2017**, *358* (6365), 868–870. https://doi.org/10.1126/science.aao6711.

(4) Schwartz, T. J.; Shanks, B. H.; Dumesic, J. A. Coupling Chemical and Biological Catalysis: A Flexible Paradigm for Producing Biobased Chemicals. *Curr. Opin. Biotechnol.* **2016**, *38*, 54–62. https://doi.org/10.1016/j.copbio.2015.12.017.

(5) Williams, C. L.; Chang, C.-C.; Do, P.; Nikbin, N.; Caratzoulas, S.; Vlachos, D. G.; Lobo, R. F.; Fan, W.; Dauenhauer, P. J. Cycloaddition of Biomass-Derived Furans for Catalytic Production of Renewable p -Xylene. *ACS Catal.* **2012**, *2* (6), 935–939. https://doi.org/10.1021/cs300011a.

(6) Green, S. K.; Patet, R. E.; Nikbin, N.; Williams, C. L.; Chang, C.-C.; Yu, J.; Gorte, R. J.; Caratzoulas, S.; Fan, W.; Vlachos, D. G.; Dauenhauer, P. J. Diels–Alder Cycloaddition of 2-Methylfuran and Ethylene for Renewable Toluene. *"Applied Catal. B, Environ.* **2016**, *180*, 487–496. https://doi.org/10.1016/j.apcatb.2015.06.044.

(7) Abdelrahman, O. A.; Park, D. S.; Vinter, K. P.; Spanjers, C. S.; Ren, L.; Cho, H. J.; Vlachos, D. G.; Fan, W.; Tsapatsis, M.; Dauenhauer, P. J. Biomass-Derived Butadiene by Dehydra-Decyclization of Tetrahydrofuran. *ACS Sustain. Chem. Eng.* **2017**, *5* (5), 3732–3736. https://doi.org/10.1021/acssuschemeng.7b00745.

(8) Abdelrahman, O. A.; Park, D. S.; Vinter, K. P.; Spanjers, C. S.; Ren, L.; Cho, H. J.; Zhang, K.; Fan, W.; Tsapatsis, M.; Dauenhauer, P. J. Renewable Isoprene by Sequential Hydrogenation of Itaconic Acid and Dehydra-Decyclization of 3-Methyl-Tetrahydrofuran. *ACS Catal.* **2017**, *7* (2), 1428–1431. https://doi.org/10.1021/acscatal.6b03335.

(9) Harmsen, P. F. H.; Hackmann, M. M.; Bos, H. L. Green Building Blocks for Bio-Based Plastics. *Biofuels, Bioprod. Biorefining* **2014**, *8* (3), 306–324. https://doi.org/10.1002/bbb.1468.

(10) Hulea, V. Toward Platform Chemicals from Bio-Based Ethylene: Heterogeneous Catalysts and Processes. *ACS Catal.* **2018**, *8* (4), 3263–3279. https://doi.org/10.1021/acscatal.7b04294.

(11) Darabi Mahboub, M. J.; Dubois, J. L.; Cavani, F.; Rostamizadeh, M.; Patience, G. S. Catalysis for the Synthesis of Methacrylic Acid and Methyl Methacrylate. *Chem. Soc. Rev.* **2018**, *47* (20), 7703–7738. https://doi.org/10.1039/c8cs00117k.

(12) Brydson, J. A. Acrylic Plastics. In *Plastics Materials*; Elsevier, 1999; pp 398–424. https://doi.org/10.1016/B978-075064132-6/50056-5.

(13) Pawar, E. A Review Article on Acrylic PMMA Eshwar Pawar. *ISOR J. Mech. Civ. Eng.* **2016**, *13* (2), 1–4. https://doi.org/10.9790/1684-1302010104.

(14) Takaki, A.; Yasui, H.; Narisawa, I. Fracture and Impact Strength of Poly(Vinyl Chloride)/Methyl Methacrylate/Butadiene/Styrene Polymer Blends. *Polym. Eng. Sci.* **1997**, *37* (1), 105–119. https://doi.org/10.1002/pen.11651.

(15) LG Chem. Polymethyl Methacrylate & Styrene-Methyl Methacrylate Copolymer. **2017**.

(16) Nagai, K. New Developments in the Production of Methyl Methacrylate. *Appl. Catal. A Gen.* **2001**, *221* (1–2), 367–377. https://doi.org/10.1016/S0926-860X(01)00810-9.

(17) Lebeau, J.; Efromson, J. P.; Lynch, M. D. A Review of the Biotechnological Production of Methacrylic Acid. *Front. Bioeng. Biotechnol.* **2020**, *8* (March), 1–10. https://doi.org/10.3389/fbioe.2020.00207.

(18) Fouilloux, H.; Thomas, C. M. Production and Polymerization of Biobased Acrylates and Analogs. *Macromol. Rapid Commun.* **2021**, *42* (3). https://doi.org/10.1002/marc.202000530.

(19) Ansteinsson, V.; Kopperud, H. B.; Morisbak, E.; Samuelsen, J. T. Cell Toxicity of Methacrylate Monomers-The Role of Glutathione Adduct Formation. *J. Biomed. Mater. Res. - Part A* **2013**, *101* (12), 3504–3510. https://doi.org/10.1002/jbm.a.34652.

(20) Shaw, A. J.; Lam, F. H.; Hamilton, M.; Consiglio, A.; MacEwen, K.; Brevnova, E. E.; Greenhagen, E.; LaTouf, W. G.; South, C. R.; Van Dijken, H.; Stephanopoulos, G. Metabolic Engineering of Microbial Competitive

Advantage for Industrial Fermentation Processes. *Science (80-.).* **2016**, *353* (6299), 583–586. https://doi.org/10.1126/science.aaf6159.
(21) Grabow, L. C.; Mavrikakis, M. Mechanism of Methanol Synthesis on Cu through CO2 and CO Hydrogenation. *ACS Catal.* **2011**, *1* (4), 365–384. https://doi.org/10.1021/cs200055d.
(22) Martínez-Suarez, L.; Siemer, N.; Frenzel, J.; Marx, D. Reaction Network of Methanol Synthesis over Cu/ZnO Nanocatalysts. *ACS Catal.* **2015**, *5* (7), 4201–4218. https://doi.org/10.1021/acscatal.5b00442.
(23) Weitz, S.; Hermann, M.; Linder, S.; Bengelsdorf, F. R.; Takors, R.; Dürre, P. Isobutanol Production by Autotrophic Acetogenic Bacteria. *Front. Bioeng. Biotechnol.* **2021**, *9*. https://doi.org/10.3389/fbioe.2021.657253.
(24) Dedov, A. G.; Karavaev, A. A.; Loktev, A. S.; Mitinenko, A. S.; Moiseev, I. I. Isobutanol Conversion to Petrochemicals Using MFI-Based Catalysts Synthesized by a Hydrothermal-Microwave Method. *Catal. Today* **2021**, *367*, 199–204. https://doi.org/10.1016/j.cattod.2020.04.064.
(25) Schmidt, L. D.; Dauenhauer, P. J. NEWS & VIEWS Hybrid Routes to Biofuels. **2007**, *447* (June).
(26) Kuenz, A.; Krull, S. Biotechnological Production of Itaconic Acid—Things You Have to Know. *Appl. Microbiol. Biotechnol.* **2018**, *102* (9), 3901–3914. https://doi.org/10.1007/s00253-018-8895-7.
(27) Bafana, R.; Pandey, R. A. New Approaches for Itaconic Acid Production: Bottlenecks and Possible Remedies. *Crit. Rev. Biotechnol.* **2018**, *38* (1), 68–82. https://doi.org/10.1080/07388551.2017.1312268.
(28) Komáromy, P.; Bakonyi, P.; Kucska, A.; Tóth, G.; Gubicza, L.; Bélafi-Bakó, K.; Nemestóthy, N. Optimized PH and Its Control Strategy Lead to Enhanced Itaconic Acid Fermentation by Aspergillus Terreus on Glucose Substrate. *Fermentation* **2019**, *5* (2). https://doi.org/10.3390/fermentation5020031.
(29) Le Nôtre, J.; Witte-van Dijk, S. C. M.; van Haveren, J.; Scott, E. L.; Sanders, J. P. M. Synthesis of Bio-Based Methacrylic Acid by Decarboxylation of Itaconic Acid and Citric Acid Catalyzed by Solid Transition-Metal Catalysts. *ChemSusChem* **2014**, *7* (9), 2712–2720. https://doi.org/10.1002/cssc.201402117.
(30) Lansing, J. C.; Murray, R. E.; Moser, B. R. Biobased Methacrylic Acid via Selective Catalytic Decarboxylation of Itaconic Acid. *ACS Sustain. Chem. Eng.* **2017**, *5* (4), 3132–3140. https://doi.org/10.1021/acssuschemeng.6b02926.
(31) McCoy, M. European Biotechs Eye Itaconic Acid. *Chem. Eng. News* **2015**, *93* (41), 16–17.
(32) Alex Scott. Partners to Develop Itaconic Polymers. *C&EN Glob. Enterp.* **2017**, *95* (6), 12–13. https://doi.org/10.1021/cen-09506-buscon004.
(33) Hosseinpour Tehrani, H.; Becker, J.; Bator, I.; Saur, K.; Meyer, S.; Rodrigues Lóia, A. C.; Blank, L. M.; Wierckx, N. Integrated Strain- And Process Design Enable Production of 220 g L-1 Itaconic Acid with Ustilago Maydis. *Biotechnol. Biofuels* **2019**, *12* (1), 1–11. https://doi.org/10.1186/s13068-019-1605-6.
(34) Noh, M. H.; Lim, H. G.; Woo, S. H.; Song, J.; Jung, G. Y. Production of Itaconic Acid from Acetate by Engineering Acid-Tolerant Escherichia Coli W. *Biotechnol. Bioeng.* **2018**, *115* (3), 729–738. https://doi.org/10.1002/bit.26508.
(35) Bohre, A.; Novak, U.; Grilc, M.; Likozar, B. Synthesis of Bio-Based Methacrylic Acid from Biomass-Derived Itaconic Acid over Barium Hexa-Aluminate Catalyst by Selective Decarboxylation Reaction. *Mol. Catal.* **2019**, *476* (July). https://doi.org/10.1016/j.mcat.2019.110520.
(36) Webb, J. P.; Arnold, S. A.; Baxter, S.; Hall, S. J.; Eastham, G.; Stephens, G. Efficient Bio-Production of Citramalate Using an Engineered Escherichia Coli Strain. *Microbiol. (United Kingdom)* **2018**, *164* (2), 133–141. https://doi.org/10.1099/mic.0.000581.
(37) Parimi, N. S.; Durie, I. A.; Wu, X.; Niyas, A. M. M.; Eiteman, M. A. Eliminating Acetate Formation Improves Citramalate Production by Metabolically Engineered Escherichia Coli. *Microb. Cell Fact.* **2017**, *16* (1), 1–10. https://doi.org/10.1186/s12934-017-0729-2.
(38) Wu, X.; Eiteman, M. A. Production of Citramalate by Metabolically Engineered Escherichia Coli. **2016**, *113* (12), 2670–2675. https://doi.org/10.1002/bit.26035.
(39) Baba, T.; Ara, T.; Hasegawa, M.; Takai, Y.; Okumura, Y.; Baba, M.; Datsenko, K. A.; Tomita, M.; Wanner, B. L.; Mori, H. Construction of Escherichia Coli K-12 in-Frame, Single-Gene Knockout Mutants: The Keio Collection. *Mol. Syst. Biol.* **2006**, *2*. https://doi.org/10.1038/msb4100050.
(40) Miller, J. H. *Experiments in Molecular Genetics*; Cold Spring Harbor Laboratory,

1972.
(41) Lundberg, D. J.; Lundberg, D. J.; Zhang, K.; Dauenhauer, P. J. Process Design and Economic Analysis of Renewable Isoprene from Biomass via Mesaconic Acid. *ACS Sustain. Chem. Eng.* **2019**, *7* (5), 5576–5586. https://doi.org/10.1021/acssuschemeng.9b00362.
(42) Kuznetsov, A.; Kumar, G.; Ardagh, M. A.; Tsapatsis, M.; Zhang, Q.; Dauenhauer, P. J. On the Economics and Process Design of Renewable Butadiene from Biomass-Derived Furfural. *ACS Sustain. Chem. Eng.* **2020**, *8* (8), 3273–3282. https://doi.org/10.1021/acssuschemeng.9b06881.
(43) Lundberg, D. J.; Lundberg, D. J.; Hillmyer, M. A.; Dauenhauer, P. J. Techno-Economic Analysis of a Chemical Process to Manufacture Methyl-Îμ -Caprolactone from Cresols. *ACS Sustain. Chem. Eng.* **2018**, *6* (11), 15316–15324. https://doi.org/10.1021/acssuschemeng.8b03774.
(44) Atsumi, S.; Liao, J. C. Directed Evolution of Methanococcus Jannaschii Citramalate Synthase for Biosynthesis of 1-Propanol and 1-Butanol by Escherichia Coli. *Appl. Environ. Microbiol.* **2008**, *74* (24), 7802–7808. https://doi.org/10.1128/AEM.02046-08.
(45) Nakano, K.; Rischke, M.; Sato, S.; Märkl, H. Influence of Acetic Acid on the Growth of Escherichia Coli K12 during High-Cell-Density Cultivation in a Dialysis Reactor. *Appl. Microbiol. Biotechnol.* **1997**, *48* (5), 597–601. https://doi.org/10.1007/s002530051101.
(46) Phue, J. N.; Lee, S. J.; Kaufman, J. B.; Negrete, A.; Shiloach, J. Acetate Accumulation through Alternative Metabolic Pathways in AckA-Pta-PoxB- Triple Mutant in E. Coli B (BL21). *Biotechnol. Lett.* **2010**, *32* (12), 1897–1903. https://doi.org/10.1007/s10529-010-0369-7.
(47) Harder, B. J.; Bettenbrock, K.; Klamt, S. Model-Based Metabolic Engineering Enables High Yield Itaconic Acid Production by Escherichia Coli. *Metab. Eng.* **2016**, *38*, 29–37. https://doi.org/10.1016/j.ymben.2016.05.008.
(48) Wang, J.; Wang, J.; Tai, Y. shu; Zhang, Q.; Bai, W.; Zhang, K. Rerouting Carbon Flux for Optimized Biosynthesis of Mesaconate in Escherichia Coli. *Appl. Microbiol. Biotechnol.* **2018**, *102* (17), 7377–7388. https://doi.org/10.1007/s00253-018-9135-x.
(49) Krull, S.; Hevekerl, A.; Kuenz, A.; Prüße, U. Process Development of Itaconic Acid Production by a Natural Wild Type Strain of Aspergillus Terreus to Reach Industrially Relevant Final Titers. *Appl. Microbiol. Biotechnol.* **2017**, *101* (10), 4063–4072. https://doi.org/10.1007/s00253-017-8192-x.
(50) Yu, C.; Cao, Y.; Zou, H.; Xian, M. Metabolic Engineering of Escherichia Coli for Biotechnological Production of High-Value Organic Acids and Alcohols. *Appl. Microbiol. Biotechnol.* **2011**, *89* (3), 573–583. https://doi.org/10.1007/s00253-010-2970-z.
(51) Hevekerl, A.; Kuenz, A.; Vorlop, K. D. Filamentous Fungi in Microtiter Plates - An Easy Way to Optimize Itaconic Acid Production with Aspergillus Terreus. *Appl. Microbiol. Biotechnol.* **2014**, *98* (16), 6983–6989. https://doi.org/10.1007/s00253-014-5743-2.
(52) Li, J.; Brill, T. B. Spectroscopy of Hydrothermal Solutions 18: PH-Dependent Kinetics of Itaconic Acid Reactions in Real Time. *J. Phys. Chem. A* **2001**, *105* (48), 10839–10845. https://doi.org/10.1021/jp012501s.
(53) Immer, J. G.; Kelly, M. J.; Lamb, H. H. Catalytic Reaction Pathways in Liquid-Phase Deoxygenation of C18 Free Fatty Acids. *Appl. Catal. A Gen.* **2010**, *375* (1), 134–139. https://doi.org/10.1016/j.apcata.2009.12.028.
(54) Carlsson, M.; Habenicht, C.; Kam, L. C.; Antal, M. J.; Bian, N.; Cunningham, R. J.; Jones, M. Study of the Sequential Conversion of Citric to Itaconic to Methacrylic Acid in Near-Critical and Supercritical Water. *Ind. Eng. Chem. Res.* **1994**, *33* (8), 1989–1996. https://doi.org/10.1021/ie00032a014.
(55) Kreyenschulte, D.; Heyman, B.; Eggert, A.; Maßmann, T.; Kalvelage, C.; Kossack, R.; Regestein, L.; Jupke, A.; Büchs, J. In Situ Reactive Extraction of Itaconic Acid during Fermentation of Aspergillus Terreus. *Biochem. Eng. J.* **2018**, *135*, 133–141. https://doi.org/10.1016/j.bej.2018.04.014.
(56) Datsenko, K. A.; Wanner, B. L. One-Step Inactivation of Chromosomal Genes in Escherichia Coli K-12 Using PCR Products. *Proc. Natl. Acad. Sci. U. S. A.* **2000**, *97* (12), 6640–6645. https://doi.org/10.1073/pnas.120163297.